MIDDLE POMERANIAN SCIENTIFIC SOCIETY OF THE ENVIRONMENT PROTECTION
ŚRODKOWO-POMORSKIE TOWARZYSTWO NAUKOWE OCHRONY ŚRODOWISKA
Annual Set The Environment Protection
Rocznik Ochrona Środowiska
Volume/Tom 17. Year/Rok 2015 ISSN 1506-218X 300–315

Formation of CO in the Oxy-Fuel Premixed Flame

Wojciech Jerzak
AGH University of Science and Technology

1. Introduction

Combustion is a chemical process of great importance, as it provides man with energy that is necessary for carrying out everyday life activities, transport, heating houses, or generating electric power. The latest Energy Information Administration report says: The global consumption of energy from fossil fuels will grow by 56% in 2040 [8]. So, fossil fuels are going to remain the predominant energy source, while the strong economic growth of developing countries will be a driving force for the increase in energy demand. The increase in energy generation from fossil fuels will increase the emission of CO_2, among other gases. With the aim of reducing the emissions of greenhouse gases, which include e.g. N_2O, CH_4 and CO_2, studies are being conducted, which are concerned with oxy-combustion – changing the fuel oxidizer from air to oxygen [11, 18] or oxygen carriers, such as Fe_3O_4, NiO [14]; the addition of CO_2 to the flame [10]; the absorption of CO_2 by, e.g., concrete aggregate [15].

Flue gases from oxy-combustion contain chiefly CO_2 and H_2O. The capture of CO_2 from flue gas in oxygen combustion is easier than in air combustion. It is essential to equip oxy-combustion boilers with an integrated system for the separation and transfer of CO_2 to the place of its storage and isolation from the atmosphere. Flue gas carbon dioxide is partially reused as a coolant, as oxygen combustion considerably increases the flame temperature. Flue gas recirculation allows the protection of both the burners, as well as the devices that monitor, e.g., the combustion chamber temperature (such as thermocouples). The addition of CO_2 to

oxy-combustion makes it possible to achieve a volume of substrates, which is comparable to air combustion. This enables achangeover back to air combustion (flexi-burn) to be made in case of a failure of the oxygen generation plant. An additional justification for adding CO_2 to methane (the main component of natural gas) is the fact of supplying gas turbines with a CH_4-CO_2 mixture. The CH_4-CO_2 mixture may originate from the anaerobic digestion of biomass or organic industrial wastes [7].

Experimental tests and numerical studies have found that high CO_2 concentration in oxy-combustion substrates favours incomplete combustion, that is the formation of CO [2–4, 6, 13]. Due to the slow CO combustion reaction, the concentrations of carbon monoxide in the region of the oxy-fuel burner are higher than the equilibrium values for the examined residence times [6]. Moreover, the CO increases exponentially with flame temperature and decreases with increasing pressure. Glarborg and Bentzen [6] interpreted the experimental results using a detailed mechanism of hydrocarbon oxidation. They have concluded that the high CO_2 concentration around the burner prevents the complete oxidation of fuel at temperatures higher than 1200K, in spite of the presence excess of oxygen. According to reaction $CO_2 + H \leftrightarrow CO + OH$, high CO_2 concentration in the flame uses up the hydrogen radicals, thus disturbing the course of reaction $H + O_2 \leftrightarrow O + OH$. Another effect of the above-mentioned reaction is a change in the O/H radical proportion.

Experiments and numerical computations carried out using three different combustion mechanisms have shown that the peak CO concentrations in the flame during methane combustion in air increase with increasing CO_2 addition to the air-fuel mixture [6].

The addition of oxygen to combustion air contributes to a distinct shortening and a change in the shape of the flame [4]. Controlling the flame shape may prove useful for avoiding refractory material overheating in a specific location and changing the heat flux and temperature profiles in the combustion chamber.

2. Experimental section

Experiments were carried out for the combustion of natural gas with the following composition: CH_4=98%; C_2H_6=0.6%; C_3H_8=0.3%; N_2=1%; CO_2=0.1%. Combustion was conducted with a 5% excess oxygen. The following oxy-combustion atmospheres were examined: 23%O_2/77%CO_2, 25%O_2/75%CO_2; 27%O_2/73%CO_2; 29%O_2/71%CO_2. Oxygen and carbon dioxide from cylinders were passed to a gas mixer and then to a kinetic burner of a power of approx. 1kW. The burner belongs to a group of low-swirl burners, in which the degree of stream swirl is defined with the swirl number S<0.6. The stream of substrates (a natural gas/O_2/CO_2 mixture) passes through the openings in the central duct and the vanes surrounding it. Such a construction of the exchangeable radial swirler creates a low vortex flow with a stable flame. The swirler with 11 vanes and a vane inclination angle of 45^o was situated inside the burner (0.01m away from the outlet). A movable element of the measuring position was the burner, whose distances from the flue gas sampling probe was varied in the range of 0.02 – 0.1 m with a step of 0.02 m. The inner diameter of the burner was 0.022 m, while the diameter of the flue gas sampling probe was 0.004 m. The ceramic probe was distinguished by high brittleness, therefore it remained in the same place throughout the experiment period. Flue gas sampling was done in the burner's axis. Inside the ceramic probe, a 0.0005 m-diameter PtRh10-Pt thermocouple is installed. The combustion chamber, in which measurements were taken, is illustrated in Fig. 1a. The combustion chamber is composed of a ϕ = 60 quartz tube, a cylindrical resistance furnace and furnace lagging of 0.05 m-thick ceramic fibres. All tests were started in a location between the burner and the resistance furnace, 0.1 m away from the burner, and a constant temperature of 1443K was maintained in that location. Photograph 1b shows a flame with a length of approx. 0.13 m in the open space for the atmosphere 27%O_2/73%CO_2. Flue gas sampled from the flame was transferred to a cooler via the heating line, and then to an Horiba PG350 continuous duty analyzer. The measurement of CO in this device was done with a non- dispersion infrared absorption detector (NDIR). The uncertainty of measurement was about 1% of the magnitude of measured concentration.

a) 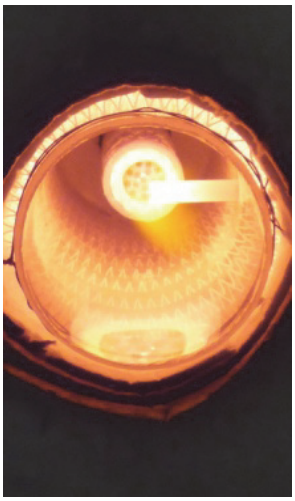 b) 

Fig. 1. A picture of the flame: a) in the combustion chamber; b) in the open space
Rys. 1. Zdjęcie płomienia: a) w komorze spalania; b) w przestrzeni otwartej

For all conditions: $\dot{V}_{fuel} = 0.08$ m^3/h; $\dot{V}_{oxygen} = 0.168$ m^3/h; $T_{oxidizer} = 300$K, $\lambda_{oxygen} = 1.05$. The tests were started from a mixture containing 29% O_2, and then CO_2 was added according to Table 1. The addition of CO_2 resulted in an increase in combustible mixture volume with a drop in oxygen content.

Table 1. Experimental conditions
Tabela 1. Warunki eksperymentalne

$\%O_2/\%CO_2$	CO_2, m^3/h	Combustible Mixture, m^3/h
23/77	0.562	0.81
25/75	0.504	0.75
27/73	0.454	0.7
29/71	0.411	0.657

The flame with the addition of 29% O_2 is less visible, as its colour becomes identical to that of the heated chamber lining. When the proportion of O_2 to CO_2 has decreased, the flame becomes clearly shining.

3. Numerical approach

The description of reactions occurring in the flame is extremely difficult and depends on numerous factors, such as temperature, pressure, burner type, fuel and oxidizing mixture compositions, etc. Depending the number of reagents and their stoichiometric coefficients, first-, second- and third-order reactions are distinguished.

For the general notation of the reaction:

$$\sum_{i=1}^{n} \nu_i' Z_i \overset{k}{\Rightarrow} \sum_{i=1}^{n} \nu_i'' Z_i \tag{1}$$

whose order can be expressed as follows:

$$m = \sum_{i=1}^{n} \nu_i' \tag{2}$$

the rate of production of the component Z_i of reaction (1) is

$$r_{Z_i} = \frac{dC_{Z_i}}{dt} = (\nu_i'' - \nu_i')k \prod_{i=1}^{n} \left(C_{Z_i}\right)^{\nu_i'} \tag{3}$$

The reaction rate constant k for reaction of any order is defined using the modified Arrhenius equation:

$$k = AT^{\beta} e^{-\frac{E_a}{RT}} \tag{4}$$

The resultant of the production rate is the sum for the reaction running to the left-hand and the right-hand direction, respectively:

$$[r_{Z_i}]_{Net} = [r_{Z_i}]_{Forward} + [r_{Z_i}]_{Reverse} \tag{5}$$

There are many detailed mechanism provided in the literature, which are intended for the analysis of the gaseous fuel combustion kinetics. The most popular include: GRI-Mech [17] and those developed by Konnov [12] and Mendiara, Glarborg [16]. Mechanisms are created by combining experimental results and theoretical models defining parameters in the modified reaction rate constant equation (4). The above-mentioned reaction mechanisms [12, 16, 17] differ in the number of reactions, chemical compounds and elements and the values of activation energy E_a and the constants A, β.

In the present study, modelling of the natural gas combustion kinetics was performed within the Chemked II software program, version 3.5.2 [9], using the combustion mechanism proposed by Mendiara, Glarborg [16]. The combustion mechanism includes 779 elementary reactions between 97 chemical compounds. The computations were conducted for a flame temperature of 1500K, at a constant pressure of p = 0.1 MPa. The ideal mixing of the combustion substrates in the burner was assumed for the computations.

The adiabatic equilibrium flame temperatures during the combustion of methane with the addition of O_2 and CO_2 were determined in the program FactSage™ [1]. Using the Equilib module operating based on the Gibbs free energy minimum principle, the state of thermodynamic equilibrium between reagents occurring in different states of aggregation was determined. As the criterion for the computations in the FactSage™ program, the equality of product and substrate enthalpies at a constant pressure was adopted. The computations were made for initial conditions consistent with the experiment, i.e. p = 0.1 MPa; T = 300K; $\lambda = 1.05$.

4. Computation and experiment results

Table 2 summarizes real and adiabatic flame temperatures, depending on the combustion atmosphere used. The real flame temperatures in the examined system are equal to the temperature of flue gas taken for the analysis of CO. The highest flame temperature of 1633K was noted at a distance of 0.06 m from the burner for the oxidizing atmosphere containing 29% O_2. The decrease in the oxygen fraction of the mix was followed by a shift in the maximum burner flame temperature closer to the burner, i.e. to a distance of 0.04 m. The change in the location of the maximum temperature in the kinetic low-swirl flame used may be indicative of a shortening of the flame length with the decrement of oxygen. The trend in flame length change is reverse to that for combustion in oxygen-enriched air [4]. From the computations made in the FactSage™ program it was found that the adiabatic flame temperature increased with increasing oxygen content of the oxidizing mixture from 1825K (for $23\%O_2/77\%CO_2$) to 2087K (for $29\%O_2/71\%CO_2$).

Table 2. Temperatures for different combustion atmospheres
Tabela 2. Temperatury dla różnych atmosfer spalania

$O_2/CO_2 \rightarrow$	23%/77%	25%/75%	27%/73%	29%/71%
Distance, m	Temperature, K			
0.02	1275	1358	1463	1584
0.04	1512	1543	1611	1598
0.06	1486	1512	1580	1633
0.08	1463	1497	1548	1573
0.1	1443	1443	1443	1443
$\mathbf{T_{adiabatic}, K}$	1825	1922	2009	2087

The experimentally determined variations in CO concentrations (in dry flue gas) in the flame are shown in Fig. 2. The following regularity can be observed. The increase in oxygen share in the oxy-combustion process results in a drop in CO already at a distance of 0.1 m from the burner, as marked by the broken line in Fig. 2. An opposite trend in CO concentration variations was found at a distance of 0.02 m. The farther away from the burner, the less CO in the burner region. The values of CO concentrations at particular distances from the burner oscillate within a certain concentration range. Allowing for this, two concentrations, a minimum and a maximum, are plotted at each measurement point in Figure 2. An example section of carbon monoxide variations in time, as recorded with the flue gas analyzer for the 27%O_2/73% CO_2 variant at a distance of 0.1 m from the burner outlet, is shown in Fig. 3.

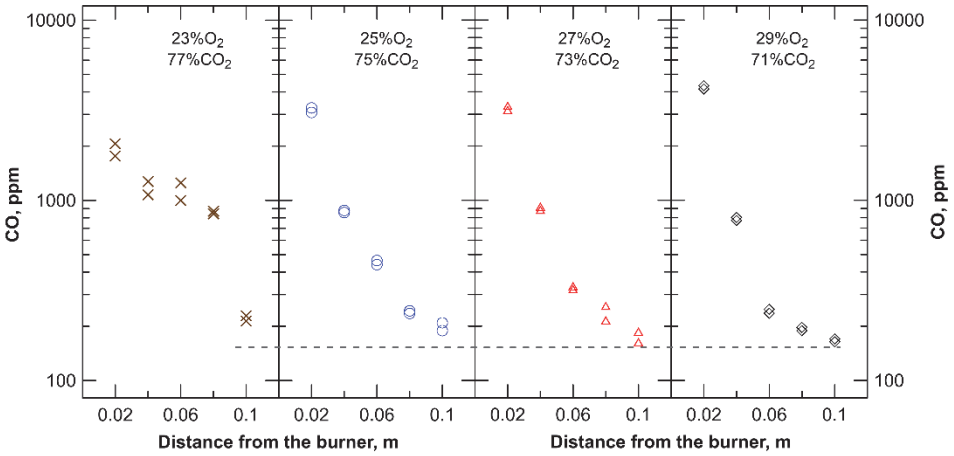

Fig. 2. CO concentration in dry flue gas for the examined variants and varying distances from the burner
Rys. 2. Stężenie CO w spalinach suchych dla rozpatrywanych wariantów i różnych odległości od palnika

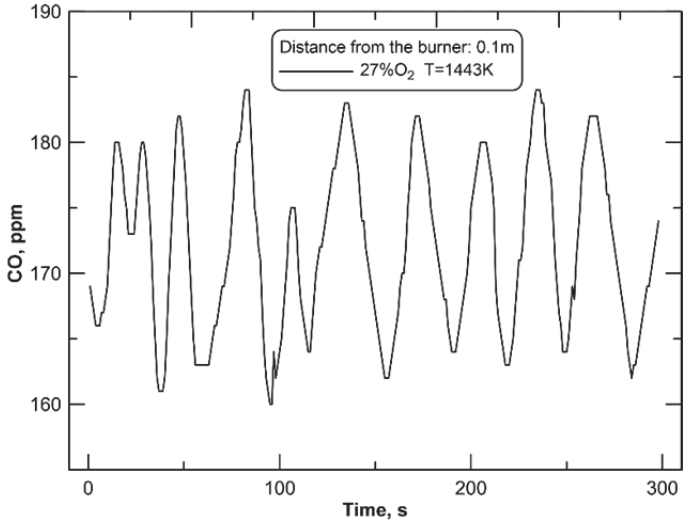

Fig. 3. Variations in CO concentration in time at a distance of 0.1 m from the burner outlet
Rys. 3. Przebieg zamian stężenia CO w czasie w odległości 0.1 m od wylotu palnika

The next figure illustrates the peak CO molar fractions (as related to dry flue gas) in the flame at a temperature of 1500K, as computed in the Chemked II program, as a function of residence time. As can be seen in Figure 4, the peak CO molar fractions form slightly faster in the conditions of a higher oxygen content of the oxidizing mixture. The maximum peak CO molar fraction value falls on the oxygen-richest atmosphere, as indicated in the magnified relevant fragment of the diagram. With the decrease in the oxygen share of the O_2/CO_2 mixture, the peak CO molar fractions decrease. The variations in CO molar fractions as a function of residence time, determined based on computations, are characterized by the same trend of changes as for the experiments. The farther away from the burner, and so the longer the residence time, the more the CO fraction grows with increasing CO_2 addition. This effect is reflected in the literature [2, 4, 5]. Carbon monoxide forms very fast in the flame in the oxy-combustion process, as indicated by its maximum concentrations in the vicinity of the burner. However, its oxidation to CO_2 is much slower, which is due to the decrease in the CO molar fractions with increasing residence time.

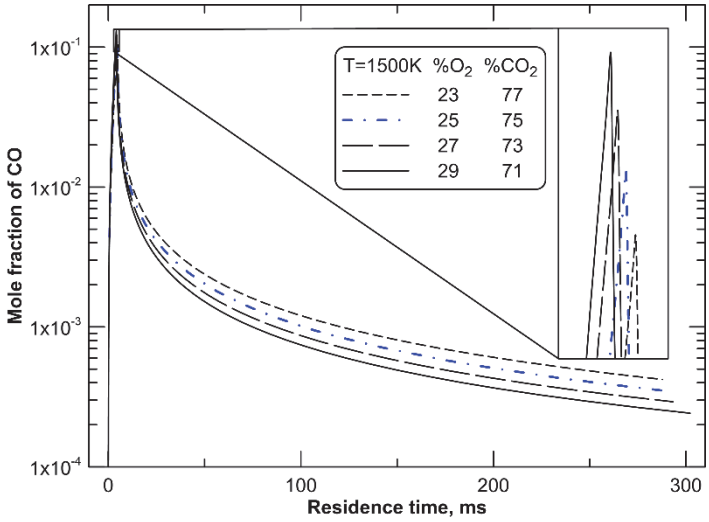

Fig. 4. The effect of residence time on the CO molar fraction for different combustion atmospheres

Rys. 4. Wpływ czasu przebywania na udział molowy CO dla różnych atmosfer spalania

The quantity of water formed in wet flue gas due to the change of combustion atmosphere is shown in Figure 5. The increase in the water molar fraction as a result of increasing the content of oxygen of the oxidizing mixture can be explained by the specificity of the conducted tests. The volume flux of combusted natural gas and oxygen is constant, so the quantity of water formed is invariable too. As a result of the addition of CO_2, the combustible mix volume is increased (according to Table 1), thus the H_2O molar fraction of the flue gas decreases.

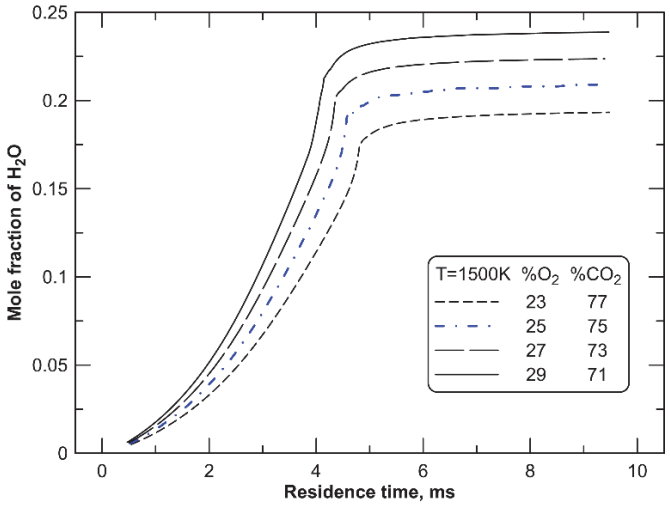

Fig. 5. The effect of residence time on the H_2O molar fraction for different combustion atmospheres
Rys. 5. Wpływ czasu przebywania na udział molowy H_2O dla różnych atmosfer spalania

Figure 6 displays the patterns of variations in CO_2 molar fractions for the examined atmospheres as a function of time. In the early phase of the diagram (0–4 ms), the CO_2 molar fraction of flame is commensurate with the content of CO_2 of the combustible mixture. This is too short time for the natural gas to be completely oxidized with the formation of water. After approx. 5 ms, the largest quantity of CO_2 (as related to dry flue gas) is for the combustible mixture $29\%O_2/71\%CO_2$ with the smallest flux of 0.657 m^3/h. Noteworthy is the short time needed for attaining a high CO_2 molar fraction of flame at a level of 0.95. In the natural gas combustion reaction, the quantities and types of free radicals formed in the flame are not without significance.

Variations in hydrogen radicals in the flame for the examined oxy-combustion atmospheres are illustrated in Fig. 7. It follows from the figure that the greater the CO_2 fraction of the combustible mixture, the smaller the magnitude of peak H molar fractions.

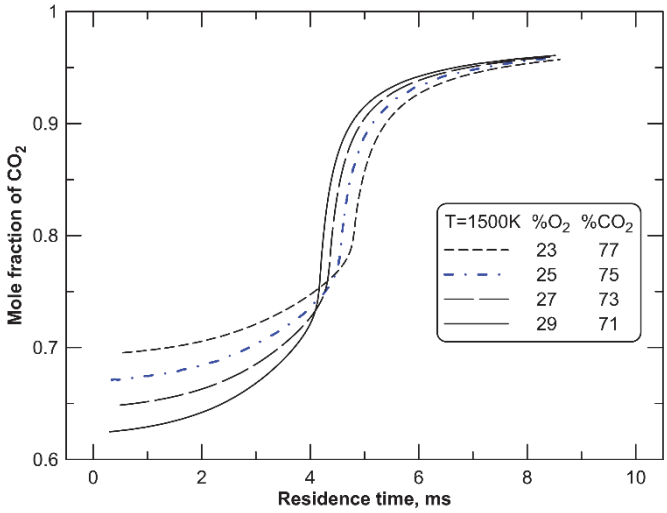

Fig. 6. The effect of residence time on the CO_2 molar fraction for different combustion atmospheres
Rys. 6. Wpływ czasu przebywania na udział molowy CO_2 dla różnych atmosfer spalania

Based on the analysis of the reaction rate in accordance with Eq. (3) at a temperature of 1500K, five predominant reactions of CO formation and consumption in the flame are listed.

$$OH + CO \leftrightarrow H + CO_2 \quad (6)$$

$$HCCO + O_2 \leftrightarrow OH + CO + CO \quad (7)$$

$$HCO + H_2O \leftrightarrow H + CO + H_2O \quad (8)$$

$$HCO + O_2 \leftrightarrow HO_2 + CO \quad (9)$$

$$H_2 + CO + M \leftrightarrow CH_2O + M \quad (10)$$

From among the above-mentioned reactions, reaction (6) contributes most to the formation of CO in the flame, which is confirmed in scientific studies [5, 6, 19]. The clear effect of the natural gas oxy-

combustion atmosphere on the rate of reaction (6) of CO formation and consumption in the flame is demonstrated in Fig. 8. The greater oxygen fraction of the combustible mixture increases the net CO formation rate according to Eq. (5). Favourable conditions for the formation of CO in the flame following reaction (6) proceeding to the left include the H free radical fraction, which increases with increasing oxygen content of the combustible mix, as suggested by Fig. 7.

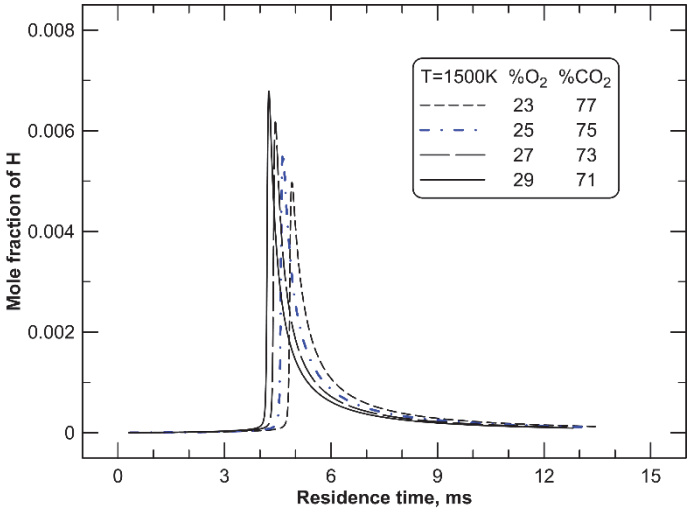

Fig. 7. The peak molar fractions of H radicals for different combustion atmospheres
Rys. 7. Szczytowe udziały molowe rodników H dla różnych atmosfer spalania

The change in the rate of reaction (6) due to the modification of the combustion atmosphere not only results in an increase in CO in the flame region, but also disturbs the proportions of free radicals in the flame. Though belonging to unstable intermediate products, H, OH or H radicals are responsible for the initiation, branching, propagation and termination of reaction chains.

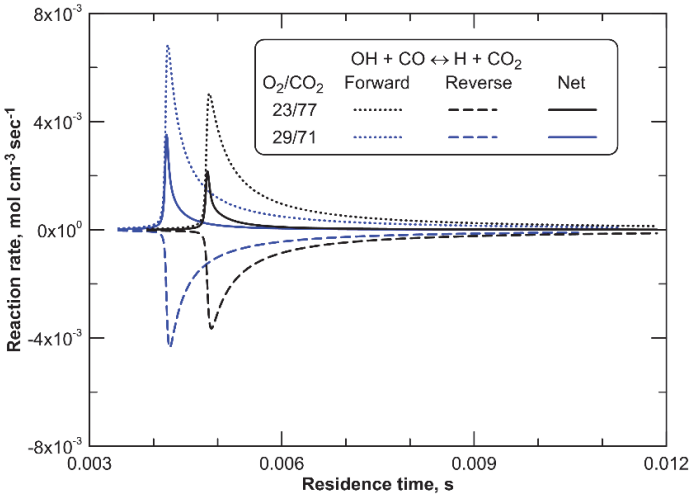

Fig. 8. The rate of reaction (6) for different combustion atmospheres
Rys. 8. Szybkość reakcji (6) dla różnych atmosfer spalania

5. Conclusions

Computations and experiments concerning the oxy-combustion of natural gas preliminarily mixed with CO_2 and 23–29 vol.% O_2 have been carried out. The richer the atmosphere,

1. the higher the magnitude of adiabatic flame temperature,
2. the higher the peak CO molar fractions at a small distance from the burner,
3. the smaller the CO molar fraction at greater distances from the burner,
4. the more H radicals are formed,
5. the lower the rate of the predominant CO formation reactions.

Many reactions are responsible for the formation of CO in the flame, with the primary being: $OH + CO \leftrightarrow H + CO_2$.

A reaction classified as second in terms of CO formation rate is: $HCCO + O_2 \leftrightarrow OH + CO + CO$.

Carbon monoxide forms very fast in the flame in the oxy-combustion process, as indicated by its maximum concentrations in the vicinity of the burner. However, the oxidation of carbon monoxide to CO_2 is much slower, which is due to the decrease in the CO molar fractions with increasing residence time. The presence of CO_2 in the combustion substrates has an inhibiting effect on the fuel oxidation process.

Acknowledgements

The author thank Mr. Piotr Mondkiewicz from the Department of Heat Engineering and Environment Protection for technical assistance in the experiments.

The work was supported by grant no. AGH: 15.11.110.234

List of symbols:

A – pre-exponential factor, $(cm^3\ mol^{-1})^{m-1}s^{-1}$
C – concentration, mol cm^{-3}
E_a – activation energy of a chemical reaction, J mol^{-1}
i – number of reactions,
k – reaction rate coefficient, $(cm^3\ mol^{-1})^{m-1}s^{-1}$
m_i – order of a reaction,-
M – third body, -
r_i – rate of reaction, mol $cm^{-3}\ s^{-1}$
R – ideal gas constant, J $mol^{-1}\ K^{-1}$
S – swirl number, -
T – temperature, K
Z_i – chemical symbol „i”

Greek symbols:

β – temperature exponent of the pre-exponential factor, -
λ – excess of oxygen, -
v_i' – the stoichiometric ratio of the substrate in the reaction, -
v_i'' – the stoichiometric ratio of the reaction product, -

References

1. **Bale C.W., Bélisle E., Chartrand P., Decterov S.A., Eriksson G., Hack K., Jung I.-H., Kang Y.-B., Melançon J., Pelton A.D., Robelin C., Petersen S.:** *FactSage thermochemical software and databases – recent developments.* Calphad, 2(33), 295–311 (2009).
2. **Barbas M., Costa M., Vranckx S., Fernandes R. X.:** *Experimental and chemical kinetic study of CO and NO formation in oxy-methane premixed laminar flames doped with NH_3.* Combustion and Flame, 162, 1294–1303 (2015).
3. **Baukal C. E. (ed.):** *Industrial Burners Handbook.* CRC Press LLC, Boca Raton 2003.

4. **Biett J., Deflau J.L., Pillier L., Vovelle C.:** *Influlence of CO_2 and H_2 on the Chemical Structure of a Premixed, Lean Methane-Air Flame.* Proceedings of the 3rd European Combustion Meeting. Greece 2007.
5. **Chen L., Ghoniema A. F.:** *Modeling CO_2 Chemical Effects on CO Formation in Oxy-Fuel Diffusion Flames Using Detailed, Quasi-Global, and Global Reaction Mechanisms.* Combustion Science and Technology, 186(7), 829–848 (2014).
6. **Glarborg P. and Bentzen L. B.:** *Chemical Effect of a High CO_2 Concentration in Oxy-Fuel Combustion of Methane.* Energy & Fuels, 22(1), 291–296 (2008).
7. **Gökalp I., Lebas E.:** *Alternative fuels for industrial gas turbines*. Applied Thermal Engineering, 24(11–12), 1655–1663 (2004).
8. International Energy Outlook. World Energy Outlook. 2013, July 25, www.eia.gov/forecasts/ieo/
9. **Jelezniak M., Jelezniak I.:** *Chemked-II version 3.5. Program for chemical kinetics of gas-phase reactions*. http://www.chemked.com
10. **Jerzak W.:** *Emissions of NO_x and CO from natural gas combustion with adding CO_2 at varying distances from the burner.* Rocznik Ochrona Środowiska (Annual Set The Environment Protection), 16, 148–160 (2014).
11. **Kalicka Z., Jerzak W. Kawecka Cebula E.:** *The effect of combustion of natural gas with 21-29% $O_2/CO_2/N_2$ mixtures on emission of carbon monoxide.* Archives of Environmental Protection, 39(4), 93–103 (2013).
12. **Konnov A.A.:** *Remaining uncertainties in the kinetic mechanism of hydrogen combustion.* Combustion and Flame. 152(4), 507–528 (2008).
13. **Li G., Zhou H., Cen K.:** *Emission characteristics and combustion instabilities in an oxy-fuel swirl-stabilized combustor.* Journal of Zhejiang University SCIENCE A, 9(11), 1582–1589 (2008).
14. **Lyngfelt A., Leckner B., Mattisson T.:** *A fluidized-bed combustion process with inherent CO_2 separation; application of chemical-looping combustion.* Chemical Engineering Science, 56(10), 3101–3113 (2001).
15. **Mądrawski J., Ziemblińska K., Juszczak R., Zawal D., Olejnik J.:** *Tradycyjne i alternatywne metody oceny intensywności procesu sekwestracji ditlenku węgla przez kruszywo betonowe z recyklingu.* Rocznik Ochrona Środowiska (Annual Set The Environment Protection), 15, 2526–2545 (2013).
16. **Mendiara T., Glarborg P.:** *Ammonia chemistry in oxy-fuel combustion of methane*. Combustion and Flame, 156(10), 1937–1949 (2009).
17. **Smith G.P., Golden D.M., Frenklach M., Moriarty N.W., Eiteneer B., Goldenberg M., Bowman C.T., Hanson R.K., Song S., Gardiner W.C., Lissianski V.V., Qin Z.:** *Gri-Mech™*, www.me.berkeley.edu/gri_mech
18. **Toftegaard M.B., Brixa J., Jensena P.A., Glarborg P., Jensen A.D.:** *Oxy-fuel combustion of solid fuels.* Progress in Energy and Combustion Science, 36(5), 581–625 (2010).

19. **Xie Y., Wang J., Zhang M., Gong J., Jin W., Huang Z.:** *Experimental and Numerical Study on Laminar Flame Characteristics of Methane Oxy-fuel Mixtures Highly Diluted with CO_2.* Energy & Fuels, 27, 6231–6237 (2013).

Powstawanie CO w kinetycznym płomieniu tlenowo-paliwowym

Streszczenie

W pracy przedstawiono wyniki badań eksperymentalnych oraz numerycznych dotyczących tworzenia tlenku węgla (II) w kinetycznym płomieniu gazu ziemnego w warunkach oksy-spalania. W doświadczeniach korzystano z palnika nisko-wirowego, w którym stopień zawirowania strugi określony za pomocą liczby wiru S < 0,6. Badano wpływ składu utleniacza zawierającego CO_2 i 23–29% obj. O_2 na zmiany stężeń CO w płomieniu. Pobór spalin do analizy realizowano w osi palnika w odległościach 0,02–0,1 m z krokiem 0,02 m. Pomiaru temperatury spalin zasysanych do analizy dokonano termoparą PtRh10-Pt.

Analizę reakcji w płomieniu o temperaturze 1500K przeprowadzono w programie Chemked II [7], po zaimplementowaniu mechanizmu spalania zaproponowanego przez Mendiara, Glarborg [14] zawierającego 779 reakcji zachodzących pomiędzy 97 związkami chemicznymi. W pakiecie FactSage™ [1] obliczono adiabatyczne równowagowe temperatury płomieni podczas spalania gazu ziemnego z dodatkiem O_2 i CO_2.

Na podstawie obliczeń w programie Chemked wytypowano dominujące reakcje odpowiedzialne za tworzenie CO w płomieniu. Największy wkład w tworzenie CO ma reakcja: $OH + CO \leftrightarrow H + CO_2$, a jej szybkość jest uzależniona od udziału CO_2 w atmosferze utleniającej. Drugą reakcją sklasyfikowaną wg szybkości tworzenia CO jest: $HCCO + O_2 \leftrightarrow OH + CO + CO$.

Ponadto określono szczytowe stężenia rodników H, biorące udział w reakcjach tworzenia CO przy współudziale CO_2 oraz ich zmiany z zawartością tlenu w mieszance palnej.

Tlenek węgla w procesie oksy-spalania powstaje w płomieniu bardzo szybko, o czym świadczą szczytowe stężenia CO występujące najbliżej palnika. Jednak jego utlenienie do CO_2 jest znacznie wolniejsze co wynika ze spadku stężenia CO z czasem rezydencji. Obecność znacznych ilości CO_2 w substratach spalania ma działanie hamujące proces utleniania gazu ziemnego.

Słowa kluczowe:
oksy-spalanie, stężenie CO w płomieniu, kinetyka spalania

Keywords:
oxy-combustion, flame CO concentration, combustion kinetics